PERGAMON

International Journal of Solids and Structures 39 (2002) 5325–5344

INTERNATIONAL JOURNAL OF SOLIDS and STRUCTURES

www.elsevier.com/locate/ijsolstr

A high order theory for functionally graded piezoelectric shells

Xiao-Hong Wu, Changqing Chen, Ya-Peng Shen *, Xiao-Geng Tian

The State Key Laboratory of Mechanical Structural Strength and Vibration, Xi'an Jiaotong University, 710049 Xi'an, China

Received 26 August 2001; received in revised form 24 June 2002

Abstract

A high order theory is presented to examine the electromechanical behavior of piezoelectric generic shells with graded material properties in the thickness direction. Different types of charge equations, depending upon whether the driving signal of piezoelectrics is free charge or electric voltage, have been derived. The obtained equations can be readily reduced to typical structures, such as beams, plates and circular cylindrical shells. The high order theory has been used to study the sensing and actuating behavior of a simply supported inhomogeneous piezoelectric circular cylindrical shell and, for comparison and validation purposes, a homogeneous shell. Comparison between the obtained numerical results to those available exact solutions for homogeneous shell shows that the developed theory is accurate. The effects of graded material properties on the piezoelectrically induced displacements, stresses, electric potential and electric displacements distributions are also quantified, clearly showing the advantage of functionally graded piezoelectrics over homogeneous ones in terms of the usages as sensors and actuators.

Keywords: Functionally graded; High order theory; Piezoelectric; Generic shell

1. Introduction

In recent years, the use of functionally graded materials (FGMs) has gained intensive attention especially in extreme high temperature environment, as reflected in numerous papers on this subject (e.g., Niino, 1990; Koizumi, 1993; Reddy and Chin, 1998). FGMs are inhomogeneous materials of which the material properties vary continuously in one (or more) direction(s). This is achieved by gradually changing the composition of the constituent materials along one direction, usually the thickness direction from one surface to another, to obtain smooth variation of material properties and optimum response to externally applied thermo-mechanical loading. FGMs are developed now for the general use as structural components in high temperature environments and being strongly considered as a potential structural material candidate for future high-speed spacecraft. Typical FGMs are made from a mixture of ceramic and metal, or a combination of different metals or different ceramics that are appropriate to achieve the desired objective.

The concept of FGMs has been applied to electronics, optics, chemistry, biomedical and many other fields. For intance, FGMs with a gradient of piezoelectric properties can be used for ultrasonic transducers

* Corresponding author. Tel.: +86-29-266-8751; fax: +86-29-323-7910.
E-mail address: ypshen@mail.xjtu.edu.cn (Y.-P. Shen).

0020-7683/02/$ - see front matter © 2002 Elsevier Science Ltd. All rights reserved.
PII: S0020-7683(02)00418-3

or, as a natural application, for bending actuators (Zhu and Meng, 1996). Typical piezoelectric ceramic actuators include unimorph benders, bimorph benders and flextensional composite structures. However, those actuators usually have a non-uniform distribution of stresses or stressed metal to ceramic bonds, or both; the bonding agent may crack or peel off at low temperature and may creep at high temperature, which could lead to reliability and lifetime limitations. A better way to solve the above problems is using FGM actuators which are monolithic type piezoelectric devices without a bonding agent. The failures originated from internal debonding or from stress concentration developed in conventional bimorphs are avoided. Significantly increased durability and reliability can thus be achieved. The depth dependence of (functionally graded) piezoelectric property in PVDF films was obtained for a variety of poling conditions and field-reversal poling can be used to increase gradient activity (Marcus, 1981). A number of preparation routes have been developed in order to produce piezoelectric ceramics with a one-dimensional gradient of the chemical composition. The subsequent poling process transforms the gradient of the chemical composition into a gradient of the piezoelectric coefficients by different mechanisms. For example, a gradient of the electrical conductivity is suited, which can be realized by a gradient of dopants or a chemical reduction of one side of oxide ceramic (Wu et al., 1996).

Following exact study of the responses of piezoelectric structures (limited to simple geometries such as simply supported plate strips, rectangular plates and circular cylindrical shells) to external loading (see, for example Bisegna and Maceri, 1996; Chen et al., 1996, 1999), much effort has been devoted to the investigation of the behavior of laminated piezoelectric plates and shells, in which the material properties are piecewise constant. Sosa (1992) developed a transfer matrix approach to investigate the electromechanical coupling characteristics of infinite laminated piezoelectric plates. By extending the work of Pagano (1970) for pure elastic laminates, Heyliger (1997) presented some exact solutions for laminated piezoelectric plates. These approaches have been extended widely to the analyses of composite laminated plates and shells for different materials and loads (Xu et al., 1997; Lee and Jiang, 1996). However, the aforementioned approaches are not suitable piezoelectric plates and shells with continuously varied material properties. Reddy and Cheng (2001) obtained an asymptotic solution of a FG structure (a functionally graded plate attached on its bottom surface by a piezoelectric actuator) by using the transfer matrix formulation in combination with the asymptotic expansion. Shell structures are more complex compared to plates. So far, to the authors' knowledge, minimal or no work has been presented in the literatures for functionally graded piezoelectric shells.

For piezoelectric structures with more complex geometry, approximate while powerful analytical models of beam, plate and shell type structures are preferred in order to facilitate the engineering design. Significant progress in this direction has been achieved for the past decade. Kim and Jones (1991) and Rivory et al. (1994) independently improved the Crawley and de Luis models (1987) for piezoelectric beams. The improved models were based upon either the Bernouli–Euler beam theory or the Timoshenko beam theory and were shown in better agreement with experimental results. Tzou and his co-workers (e.g., Tzou and Gadre, 1989; Tzou and Howard, 1994) conducted a series studies on piezoelectric and thermopiezoelectric shells. Most of their studies were based on the classic shell theory. Analogous to the Mindlin plate theory, Miller and Abramovich (1995) introduced a model to accommodate the transverse shear deformation of self-sensing piezoelectric shells. Recent studies on this aspect include those by Yang (1999), Wang and Yang (2000), Bisegna and Caruso (2001), among others.

In this paper, a high order theory is presented to model the electromechanical behavior of functionally graded piezoelectric generic shells. The generalized Hamilton's principle, which incorporates different electric boundary conditions as well as mechanical boundary conditions, is utilized to obtain the governing equations of motion. Deduction of the governing equations for piezoelectric beams, plates and circular cylindrical shells from the high order piezoelectric generic shell theory is briefly discussed. In the light of the formulae presented herein, a simply supported anisotropic inhomogeneous piezoelectric circular cylindrical shell and, for comparison and validation purposes, a homogeneous shell is considered in illustrative ex-

amples. Comparison of the numerical results for the homogeneous shell with those available exact solutions shows that the derived model is satisfactory. The effects of graded material properties on the piezoelectrically induced displacements, stresses, electric potential and electric displacements distributions are also quantified.

2. The motion and electrostatics equations

Since the governing equations for beam, plate and circular cylindrical shell type structures can be deduced directly from those of generic shells, we start the derivation of the equations for piezoelectric generic shells by introducing the co-ordinated system used in this paper. Fig. 1 shows a geometric definition of the piezoelectric shell. An orthogonal curvilinear co-ordinate system defined by three unit vectors α_1, α_2, and α_3 is attached to the structure. The thickness of the shell is assumed to be $2h$. The Lame parameters and the radii of curvature related to α_1 and α_2 are denoted by A_1, A_2, R_1 and R_2, respectively, and are independent of transverse ordinate when the shell is thin, i.e., $h \ll R_1$ and $h \ll R_2$. (In the following, z and α_3 will be used simultaneously.)

Linear constitutive equations of functionally graded piezoelectric materials with thickness-graded material properties are

$$\begin{aligned} \sigma_{ij} &= C_{ijkl}\varepsilon_{kl} - e_{kij}E_k \\ D_i &= e_{ikl}\varepsilon_{kl} + \epsilon_{ik}E_k \end{aligned} \tag{1}$$

The materials property gradient is assumed to be in the thickness direction, i.e.,

$$C_{ijkl} \equiv C_{ijkl}(z); \quad e_{kij} \equiv e_{kij}(z); \quad \epsilon_{ik} \equiv \epsilon_{ik}(z) \tag{2}$$

In the general theory of shell, the strain components and the electric field components in above equations are related to the displacement components u_i $(i = 1, 2, 3)$ and the electric potential φ by the following relations:

$$\begin{aligned} \varepsilon_{11} &= \frac{\partial u_1}{A_1\partial\alpha_1} + u_2\frac{\partial A_1}{A_1A_2\partial\alpha_2} + \frac{u_3}{R_1}; \quad \varepsilon_{22} = \frac{\partial u_2}{A_2\partial\alpha_2} + u_1\frac{\partial A_2}{A_1A_2\partial\alpha_1} + \frac{u_3}{R_2} \\ \varepsilon_{33} &= \frac{\partial u_3}{\partial\alpha_3}; \quad \gamma_{23} = \frac{\partial u_2}{\partial\alpha_3} + \frac{\partial u_3}{A_2\partial\alpha_2} - \frac{u_2}{R_2} \\ \gamma_{31} &= \frac{\partial u_1}{\partial\alpha_3} + \frac{\partial u_3}{A_1\partial\alpha_1} - \frac{u_1}{R_1} \\ \gamma_{12} &= \frac{\partial u_1}{A_2\partial\alpha_2} + \frac{\partial u_2}{A_1\partial\alpha_1} - u_2\frac{\partial A_2}{A_1A_2\partial\alpha_1} - u_1\frac{\partial A_1}{A_1A_2\partial\alpha_2} \\ \gamma_{ij} &= 2\varepsilon_{ij}, \qquad i \neq j \end{aligned} \tag{3}$$

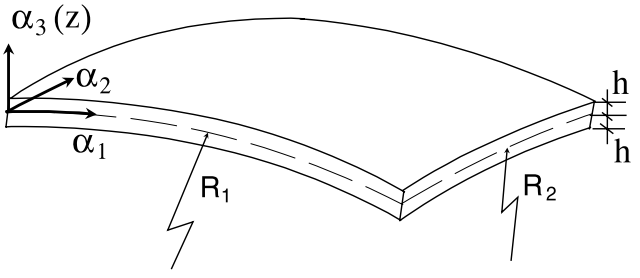

Fig. 1. Configuration of a generic piezoelectric shell.

$$E_1 = -\frac{\partial\varphi}{A_1\partial\alpha_1}; \quad E_2 = -\frac{\partial\varphi}{A_2\partial\alpha_2}; \quad E_3 = -\frac{\partial\varphi}{\partial\alpha_3} \tag{4}$$

For a piezoelectric shell subject to a prescribed surface traction $\overline{T}_i$ and a surface free charge density $\overline{w}$, the Hamilton's principle states

$$\delta\int_0^{t_1} \mathrm{d}t\left(\int_V (K-H)\,\mathrm{d}V - \int_{S_\sigma} \overline{T}_i\delta u_i\,\mathrm{d}S + \int_{S_w} \overline{w}\delta\phi\,\mathrm{d}S\right) = 0 \tag{5}$$

where

$$K\text{—kinetic density} \quad K = \tfrac{1}{2}\rho\dot{u}_i\dot{u}_i \tag{6}$$

$$H\text{—electric enthalpy density} \quad H = \tfrac{1}{2}\sigma_{ij}\varepsilon_{ij} - \tfrac{1}{2}D_iE_i \tag{7}$$

The constitutive equation (1) are related to the electric enthalpy density by

$$\sigma_{ij} = \frac{\partial H}{\partial\varepsilon_{ij}}; \quad D_i = -\frac{\partial H}{\partial E_i} \tag{8}$$

Substituting Eqs. (3), (4), (6)–(8) into Eq. (5), produces

$$\int_{t_0}^{t_1} \mathrm{d}t\left(\int_V \left(\sigma_{ij}\delta\varepsilon_{ij} + \rho\ddot{u}_i\delta u_i + D_i\delta E_i\right)\mathrm{d}V - \int_{S_\sigma} \overline{T}_i\delta u_i\,\mathrm{d}S + \int_{S_w} \overline{w}\delta\varphi\,\mathrm{d}S\right) = 0 \tag{9}$$

The equation can be further expressed as two independent equations

$$\int_V \sigma_{kl}\delta\varepsilon_{kl}\,\mathrm{d}V = -\int_V \rho\ddot{u}_i\delta u_i\,\mathrm{d}V + \int_{S_\sigma} \overline{T}_i\delta u_i\,\mathrm{d}S \tag{10}$$

$$\int_V D_k\delta E_k\,\mathrm{d}V = -\int_{S_w} \overline{w}\delta\varphi\,\mathrm{d}S \tag{11}$$

In the present theory, the displacement and the electric potential fields are assumed to be

$$\begin{aligned}
u_1(\alpha_1,\alpha_2,\alpha_3) &= u_1^{(0)}(\alpha_1,\alpha_2) + zu_1^{(1)}(\alpha_1,\alpha_2)\\
u_2(\alpha_1,\alpha_2,\alpha_3) &= u_2^{(0)}(\alpha_1,\alpha_2) + zu_2^{(1)}(\alpha_1,\alpha_2)\\
u_3(\alpha_1,\alpha_2,\alpha_3) &= u_3^{(0)}(\alpha_1,\alpha_2) + zu_3^{(1)}(\alpha_1,\alpha_2)\\
\varphi(\alpha_1,\alpha_2,\alpha_3) &= \varphi^{(0)}(\alpha_1,\alpha_2) + z\varphi^{(1)}(\alpha_1,\alpha_2) + z^2\varphi^{(2)}(\alpha_1,\alpha_2)
\end{aligned} \tag{12}$$

where $u_3^{(1)}$ is introduced to account for the transverse normal strain when the piezoelectric structure is used as actuator, and $\varphi^{(2)}$ represents the parabolic variation of the electric potential in the thickness direction. Since the assumed displacements involve linear terms and the electric potential contains both linear and quadratic terms, the developed theory is called a high order theory, compared to Mindlin type theories.

Substituting Eq. (12) into Eq. (3), yields the strain and the electric field components as

$$\begin{aligned}
&\varepsilon_{11} = \varepsilon_{11}^{(0)} + z\varepsilon_{11}^{(1)}; \quad \varepsilon_{22} = \varepsilon_{22}^{(0)} + z\varepsilon_{22}^{(1)}; \quad \varepsilon_{33} = \varepsilon_{33}^{(0)}\\
&\gamma_{23} = \gamma_{23}^{(0)} + z\gamma_{23}^{(1)}; \quad \gamma_{31} = \gamma_{31}^{(0)} + z\gamma_{31}^{(1)}; \quad \gamma_{12} = \gamma_{12}^{(0)} + z\gamma_{12}^{(1)}
\end{aligned} \tag{13}$$

$$E_1 = E_1^{(0)} + zE_1^{(1)} + z^2E_1^{(2)}; \quad E_2 = E_2^{(0)} + zE_2^{(1)} + z^2E_2^{(2)}; \quad E_3 = E_3^{(0)} + 2zE_3^{(1)} \tag{14}$$

where detail expressions for $\varepsilon_{ij}^{(0)}$, $\varepsilon_{ij}^{(1)}$ etc. can be obtained easily and are omitted for the sake of brevity.

Substituting above strain expressions into the left hand side of Eq. (10) produces

$$\begin{aligned}
\int_V \sigma_{11}\delta\varepsilon_{11}\,\mathrm{d}V &= \int_S \left[-\frac{\partial\left(A_2\sigma_{11}^{(0)}\right)}{\partial\alpha_1}\delta u_1^{(0)} + \sigma_{11}^{(0)}\frac{\partial A_1}{\partial\alpha_2}\delta u_2^{(0)} + \frac{A_1A_2}{R_1}\sigma_{11}^{(0)}\delta u_3^{(0)} - \frac{\partial\left(A_2\sigma_{11}^{(1)}\right)}{\partial\alpha_1}\delta u_1^{(1)} + \sigma_{11}^{(1)}\frac{\partial A_1}{\partial\alpha_2}\delta u_2^{(1)} \right.\\
&\quad \left. + \frac{A_1A_2}{R_1}\sigma_{11}^{(1)}\delta u_3^{(1)} \right]\mathrm{d}\alpha_1\,\mathrm{d}\alpha_2 + \int_c \left(\sigma_{11}^{(0)}n_1\delta u_1^{(0)} + \sigma_{11}^{(1)}n_1\delta u_1^{(1)}\right)\mathrm{d}c\\
\int_V \sigma_{22}\delta\varepsilon_{22}\,\mathrm{d}V &= \int_S \left[-\frac{\partial\left(A_1\sigma_{22}^{(0)}\right)}{\partial\alpha_2}\delta u_2^{(0)} + \sigma_{22}^{(0)}\frac{\partial A_2}{\partial\alpha_1}\delta u_1^{(0)} + \frac{A_1A_2}{R_2}\sigma_{22}^{(0)}\delta u_3^{(0)} - \frac{\partial\left(A_1\sigma_{22}^{(1)}\right)}{\partial\alpha_2}\delta u_2^{(1)} + \sigma_{22}^{(1)}\frac{\partial A_2}{\partial\alpha_1}\delta u_1^{(1)} \right.\\
&\quad \left. + \frac{A_1A_2}{R_2}\sigma_{22}^{(1)}\delta u_3^{(1)} \right]\mathrm{d}\alpha_1\,\mathrm{d}\alpha_2 + \int_c \left(\sigma_{22}^{(0)}n_2\delta u_2^{(0)} + \sigma_{22}^{(1)}n_2\delta u_2^{(1)}\right)\mathrm{d}c\\
\int_V \sigma_{33}\delta\varepsilon_{33}\,\mathrm{d}V &= \int_S \sigma_{33}^{(0)}\delta u_3^{(1)}A_1A_2\,\mathrm{d}\alpha_1\,\mathrm{d}\alpha_2\\
\int_V \sigma_{23}\delta\gamma_{23}\,\mathrm{d}V &= \int_S \left[-\frac{\partial\left(A_1\sigma_{23}^{(0)}\right)}{\partial\alpha_2}\delta u_3^{(0)} - \frac{\partial\left(A_1\sigma_{23}^{(1)}\right)}{\partial\alpha_2}\delta u_3^{(1)} + A_1A_2\sigma_{23}^{(0)}\delta u_2^{(0)} - \frac{A_1A_2}{R_2}\left(\sigma_{23}^{(0)}\delta u_2^{(0)} + \sigma_{23}^{(1)}\delta u_2^{(1)}\right) \right]\mathrm{d}\alpha_1\,\mathrm{d}\alpha_2\\
&\quad + \int_c \left(\sigma_{23}^{(0)}n_2\delta u_3^{(0)} + \sigma_{23}^{(1)}n_2\delta u_3^{(1)}\right)\mathrm{d}c\\
\int_V \sigma_{31}\delta\gamma_{31}\,\mathrm{d}V &= \int_S \left[-\frac{\partial\left(A_2\sigma_{31}^{(0)}\right)}{\partial\alpha_1}\delta u_3^{(0)} - \frac{\partial\left(A_2\sigma_{31}^{(1)}\right)}{\partial\alpha_1}\delta u_3^{(1)} + A_1A_2\sigma_{31}^{(0)}\delta u_1^{(0)} - \frac{A_1A_2}{R_1}\left(\sigma_{31}^{(0)}\delta u_1^{(0)} + \sigma_{31}^{(1)}\delta u_1^{(1)}\right) \right]\mathrm{d}\alpha_1\,\mathrm{d}\alpha_2\\
&\quad + \int_c \left(\sigma_{31}^{(0)}n_1\delta u_3^{(0)} + \sigma_{31}^{(1)}n_1\delta u_3^{(1)}\right)\mathrm{d}c\\
\int_V \sigma_{12}\delta\gamma_{12}\,\mathrm{d}V &= -\int_S \left[-\frac{\partial\left(A_1\sigma_{12}^{(0)}\right)}{\partial\alpha_2}\delta u_1^{(0)} - \frac{\partial\left(A_2\sigma_{12}^{(0)}\right)}{\partial\alpha_1}\delta u_2^{(0)} + \frac{\partial A_2}{\partial\alpha_1}\sigma_{12}^{(0)}\delta u_2^{(0)} + \frac{\partial A_1}{\partial\alpha_2}\sigma_{12}^{(0)}\delta u_1^{(0)} - \frac{\partial\left(A_1\sigma_{12}^{(1)}\right)}{\partial\alpha_2}\delta u_1^{(0)} \right.\\
&\quad \left. - \frac{\partial\left(A_2\sigma_{12}^{(1)}\right)}{\partial\alpha_1}\delta u_2^{(0)} + \frac{\partial A_2}{\partial\alpha_1}\sigma_{12}^{(1)}\delta u_2^{(1)} + \frac{\partial A_1}{\partial\alpha_2}\sigma_{12}^{(1)}\delta u_1^{(1)} \right]\mathrm{d}\alpha_1\,\mathrm{d}\alpha_2\\
&\quad + \int_c \left(\sigma_{12}^{(0)}n_2\delta u_1^{(0)} + \sigma_{12}^{(0)}n_1\delta u_2^{(0)} + \sigma_{12}^{(1)}n_2\delta u_1^{(1)} + \sigma_{12}^{(1)}n_1\delta u_2^{(1)}\right)\mathrm{d}c
\end{aligned} \tag{15}$$

where the infinitesimal surface area $\mathrm{d}A = \mathrm{d}\alpha_1\,\mathrm{d}\alpha_2$ is defined on the middle surface, the path integral is carried out along the contour surrounding the middle surface, and the force and moment resultants $\sigma_{kl}^{(m)}$ are given by

$$\sigma_{kl}^{(m)} = \int z^m\sigma_{kl}\,\mathrm{d}z, \quad m = 0, 1 \tag{16}$$

It is worth noting that in deriving Eq. (15), the following identities have been made use of

$$\mathrm{d}V = A_1A_2\,\mathrm{d}\alpha_1\,\mathrm{d}\alpha_2\,\mathrm{d}z; \quad 1 + z/R_1 \approx 1; \quad 1 + z/R_2 \approx 1 \tag{17}$$

Substituting Eq. (15) into Eq. (10), neglecting the body force, performing all of the integration, taking variations with respect to all variables, and collecting terms that contain variations of the same displacements, yield a system of motion equations and their corresponding boundary conditions as

$$
\begin{aligned}
&\delta u_1^{(0)}: \frac{\partial\left(A_2\sigma_{11}^{(0)}\right)}{\partial\alpha_1}+\frac{\partial\left(A_1\sigma_{12}^{(0)}\right)}{\partial\alpha_2}+\sigma_{12}^{(0)}\frac{\partial A_1}{\partial\alpha_2}-\sigma_{22}^{(0)}\frac{\partial A_2}{\partial\alpha_1}+\frac{A_1A_2}{R_1}\sigma_{31}^{(0)}+A_1A_2\left(\overline{T}_1^{+}+\overline{T}_1^{-}\right)\\
&\quad=A_1A_2\left(\rho^{(0)}\ddot{u}_1^{(0)}+\rho^{(1)}\ddot{u}_1^{(1)}\right)\sigma_{11}^{(0)}n_1+\sigma_{12}^{(0)}n_2=\overline{T}_1^{(0)}\\
&\delta u_1^{(1)}: \frac{\partial\left(A_2\sigma_{11}^{(1)}\right)}{\partial\alpha_1}+\frac{\partial\left(A_1\sigma_{12}^{(1)}\right)}{\partial\alpha_2}+\sigma_{12}^{(1)}\frac{\partial A_1}{\partial\alpha_2}-\sigma_{22}^{(1)}\frac{\partial A_2}{\partial\alpha_1}+\frac{A_1A_2}{R_1}\sigma_{31}^{(1)}-A_1A_2\sigma_{31}^{(0)}+A_1A_2\left(h\overline{T}_1^{+}-h\overline{T}_1^{-}\right)\\
&\quad=A_1A_2\left(\rho^{(1)}\ddot{u}_1^{(0)}+\rho^{(2)}\ddot{u}_1^{(1)}\right)\sigma_{11}^{(1)}n_1+\sigma_{12}^{(1)}n_2=\overline{T}_1^{(1)}\\
&\delta u_2^{(0)}: \frac{\partial\left(A_2\sigma_{12}^{(0)}\right)}{\partial\alpha_1}+\frac{\partial\left(A_1\sigma_{22}^{(0)}\right)}{\partial\alpha_2}+\sigma_{12}^{(0)}\frac{\partial A_2}{\partial\alpha_1}-\sigma_{11}^{(0)}\frac{\partial A_1}{\partial\alpha_2}+\frac{A_1A_2}{R_2}\sigma_{23}^{(0)}+A_1A_2\left(\overline{T}_2^{+}+\overline{T}_2^{-}\right)\\
&\quad=A_1A_2\left(\rho^{(0)}\ddot{u}_2^{(0)}+\rho^{(1)}\ddot{u}_2^{(1)}\right)\sigma_{12}^{(0)}n_1+\sigma_{22}^{(0)}n_2=\overline{T}_2^{(0)}\\
&\delta u_2^{(1)}: \frac{\partial\left(A_2\sigma_{12}^{(1)}\right)}{\partial\alpha_1}+\frac{\partial\left(A_1\sigma_{22}^{(1)}\right)}{\partial\alpha_2}+\sigma_{12}^{(1)}\frac{\partial A_2}{\partial\alpha_1}-\sigma_{11}^{(1)}\frac{\partial A_1}{\partial\alpha_2}+\frac{A_1A_2}{R_2}\sigma_{23}^{(1)}-A_1A_2\sigma_{23}^{(0)}+A_1A_2\left(h\overline{T}_2^{+}-h\overline{T}_2^{-}\right)\\
&\quad=A_1A_2(\rho^{(1)}\ddot{u}_2^{(0)}+\rho^{(2)}\ddot{u}_2^{(1)})\sigma_{12}^{(1)}n_1+\sigma_{22}^{(1)}n_2=\overline{T}_2^{(1)}\\
&\delta u_3^{(0)}: \frac{\partial\left(A_2\sigma_{13}^{(0)}\right)}{\partial\alpha_1}+\frac{\partial\left(A_1\sigma_{23}^{(0)}\right)}{\partial\alpha_2}-\frac{A_1A_2}{R_1}\sigma_{11}^{(0)}-\frac{A_1A_2}{R_2}\sigma_{22}^{(0)}+A_1A_2\left(\overline{T}_3^{+}+\overline{T}_3^{-}\right)\\
&\quad=A_1A_2\left(\rho^{(0)}\ddot{u}_3^{(0)}+\rho^{(1)}\ddot{u}_3^{(1)}\right)\sigma_{31}^{(0)}n_1+\sigma_{23}^{(0)}n_2=\overline{T}_3^{(0)}\\
&\delta u_3^{(1)}: \frac{\partial\left(A_2\sigma_{13}^{(1)}\right)}{\partial\alpha_1}+\frac{\partial\left(A_1\sigma_{23}^{(1)}\right)}{\partial\alpha_2}-\frac{A_1A_2}{R_1}\sigma_{11}^{(1)}-\frac{A_1A_2}{R_2}\sigma_{22}^{(1)}-A_1A_2\sigma_{33}^{(0)}+A_1A_2\left(h\overline{T}_3^{+}-h\overline{T}_3^{-}\right)\\
&\quad=A_1A_2\left(\rho^{(1)}\ddot{u}_3^{(0)}+\rho^{(2)}\ddot{u}_3^{(1)}\right)\sigma_{31}^{(1)}n_1+\sigma_{23}^{(1)}n_2=\overline{T}_3^{(1)}
\end{aligned}
\tag{18}
$$

where $\overline{T}_i^{\pm}$ refer to the surface tractions applied at the upper and lower surfaces, respectively, and $\overline{T}_i^{(m)}$ and $\rho^{(k)}$ are given by

$$
\begin{aligned}
&\overline{T}_i^{(m)}=\int\overline{T}_i z^m\,\mathrm{d}z,\quad m=0,1\\
&\rho^{(k)}=\int\rho z^k\,\mathrm{d}z,\quad k=0,1,2
\end{aligned}
\tag{19}
$$

In a similar manner, one can get the equations of electrostatics and the associated boundary conditions,

$$
\begin{aligned}
&\delta\varphi^{(0)}: \frac{\partial\left(A_2D_1^{(0)}\right)}{\partial\alpha_1}+\frac{\partial\left(A_1D_2^{(0)}\right)}{\partial\alpha_2}+A_1A_2(\overline{w}^{+}+\overline{w}^{-})=0;\quad D_1^{(0)}n_1+D_2^{(0)}n_2=\overline{w}^{(0)}\\
&\delta\varphi^{(1)}: \frac{\partial\left(A_2D_1^{(1)}\right)}{\partial\alpha_1}+\frac{\partial\left(A_1D_2^{(1)}\right)}{\partial\alpha_2}-A_1A_2D_3^{(0)}+A_1A_2(h\overline{w}^{+}-h\overline{w}^{-})=0;\quad D_1^{(1)}n_1+D_2^{(1)}n_2=\overline{w}^{(1)}\\
&\delta\varphi^{(2)}: \frac{\partial\left(A_2D_1^{(2)}\right)}{\partial\alpha_1}+\frac{\partial\left(A_1D_2^{(2)}\right)}{\partial\alpha_2}-2A_1A_2D_3^{(1)}+A_1A_2\left(h^2\overline{w}^{+}+h^2\overline{w}^{-}\right)=0;\quad D_1^{(2)}n_1+D_2^{(2)}n_2=\overline{w}^{(2)}
\end{aligned}
\tag{20}
$$

where $\overline{w}^{\pm}$ denotes the external applied surface charge densities at the upper and lower surfaces, respectively, and $D_i^{(m)}$ and $\overline{w}^{(m)}$ have the form of

$$D_i^{(m)} = \int z^m D_i \,\mathrm{d}z, \quad m = 0,1,2$$
$$\overline{w}^{(m)} = \int z^m \overline{w} \,\mathrm{d}z, \quad m = 0,1,2 \tag{21}$$

It should be emphasized that Eqs. (20) are the equations for piezoelectric sensors and piezoelectric actuator with the driving signal being electric surface free charge density. When the driving signal of piezoelectric shell actuators is electric voltage, i.e., the electric potentials on the upper and lower surfaces are prescribed, however, the corresponding electrostatics equations and their boundary conditions should be formulated in a different way. This is discussed as follows.

Denoting the prescribed electric potentials on the upper and lower surfaces by φ^+ and φ^-, respectively,

$$\varphi|_{z=h} = \varphi^+, \quad \varphi|_{z=-h} = \varphi^- \tag{22}$$

and combining the forth equation of Eq. (12), we have

$$\varphi^{(1)} = \frac{\varphi^+ - \varphi^-}{2h}, \quad \varphi^{(2)} = -\frac{\varphi^{(0)}}{h^2} + \frac{\varphi^+ + \varphi^-}{2h^2} \tag{23}$$

With Eqs. (11), (14) and (23), the electrostatics equation and its corresponding boundary condition for piezoelectric shell actuator with the electric voltage acting as the driving signal are obtained as,

$$\delta\varphi^{(0)} : \frac{\partial\left[A_2\left(D_1^{(0)} - D_1^{(2)}/h^2\right)\right]}{\partial\alpha_1} + \frac{\partial\left[A_1\left(D_2^{(0)} - D_2^{(2)}/h^2\right)\right]}{\partial\alpha_2} - \frac{2A_1A_2D_3^{(1)}}{h^2} = 0;$$
$$\left(D_1^{(0)} - D_1^{(2)}/h^2\right)n_1 + \left(D_2^{(0)} - D_2^{(2)}/h^2\right)n_2 = \overline{w}^{(0)} - \overline{w}^{(2)}/h^2 \tag{24}$$

Eq. (24) serve as alternative equations to Eq. (20) when the electric boundary conditions are specified by Eq. (22).

The constitutive relations of the shell can be obtained by integrating the constitutive Eq. (1)

$$\begin{Bmatrix} \sigma^{(0)} \\ \sigma^{(1)} \end{Bmatrix} = \begin{bmatrix} A & B \\ B & D \end{bmatrix} \begin{Bmatrix} \varepsilon^{(0)} \\ \varepsilon^{(1)} \end{Bmatrix} - \begin{bmatrix} P & Q & R \\ Q & R & H \end{bmatrix} \begin{Bmatrix} E^{(0)} \\ E^{(1)} \\ E^{(2)} \end{Bmatrix} \tag{25}$$

$$\begin{Bmatrix} D^{(0)} \\ D^{(1)} \\ D^{(2)} \end{Bmatrix} = \begin{bmatrix} P^{\mathrm{T}} & Q^{\mathrm{T}} \\ Q^{\mathrm{T}} & R^{\mathrm{T}} \\ R^{\mathrm{T}} & H^{\mathrm{T}} \end{bmatrix} \begin{Bmatrix} \varepsilon^{(0)} \\ \varepsilon^{(1)} \end{Bmatrix} + \begin{bmatrix} K & L & M \\ L & M & N \\ M & N & O \end{bmatrix} \begin{Bmatrix} E^{(0)} \\ E^{(1)} \\ E^{(2)} \end{Bmatrix} \tag{26}$$

where

$$\sigma^{(n)} = \left\{\sigma_{11}^{(n)}, \sigma_{22}^{(n)}, \sigma_{33}^{(n)}, \sigma_{23}^{(n)}, \sigma_{31}^{(n)}, \sigma_{12}^{(n)}\right\}^{\mathrm{T}}$$
$$\varepsilon^{(n)} = \left\{\varepsilon_{11}^{(n)}, \varepsilon_{22}^{(n)}, \varepsilon_{33}^{(n)}, \varepsilon_{23}^{(n)}, \varepsilon_{31}^{(n)}, \varepsilon_{12}^{(n)}\right\}^{\mathrm{T}}, \quad n = 0,1$$
$$D^{(n)} = \left\{D_1^{(n)}, D_2^{(n)}, D_3^{(n)}\right\}^{\mathrm{T}}$$
$$E^{(n)} = \left\{E_1^{(n)}, E_2^{(n)}, E_3^{(n)}\right\}^{\mathrm{T}}, \quad n = 0,1,2$$

It should be noted that the shear correction factors should be taken into account (taken to be 5/6 in the following numerical studies). The elements in the block matrices given in Eqs. (25) and (26) are defined by

$$\{A_{ij}, B_{ij}, D_{ij}\} = \int_{-h}^{h} C_{ij}\left(1, z, z^2\right)\mathrm{d}z$$
$$\{P_{ij}, Q_{ij}, R_{ij}, H_{ij}\} = \int_{-h}^{h} e_{ij}\left(1, z, z^2, z^3\right)\mathrm{d}z$$
$$\{K_{ij}, L_{ij}, M_{ij}, N_{ij}, O_{ij}\} = \int_{-h}^{h} \varepsilon_{ij}\left(1, z, z^2, z^3, z^4\right)\mathrm{d}z$$

The above definitions are valid for functionally graded piezoelectric shells. The equations of electrostatics and the related boundary conditions for the piezoelectric shells are only given when the driving signal is surface free charge density imposed upon the major surface. When the driving signal is electric voltage, the corresponding equations can be obtained straightforward.

By Substituting Eqs. (25) and (26) into Eqs. (18) and (20), the equations of motion and electrostatic in terms of displacement and electric potential can be written in compact matrix forms as

$$\begin{aligned} &L_{\mathrm{d}}U + L_{\mathrm{c}}\varphi + P = L_{\rho}\ddot{U} \\ &L_{\mathrm{c}}^{*}U + L_{\mathrm{w}}\varphi + Q = 0 \end{aligned} \tag{27}$$

where

$$U = \left\{u_1^{(0)}, u_1^{(1)}, u_2^{(0)}, u_2^{(1)}, u_3^{(0)}, u_3^{(1)}\right\}^{\mathrm{T}}$$
$$\varphi = \left\{\varphi^{(0)}, \varphi^{(1)}, \varphi^{(2)}\right\}^{\mathrm{T}}$$
$$P = \left\{P_1^{(0)}, P_1^{(1)}, P_2^{(0)}, P_2^{(1)}, P_3^{(0)}, P_3^{(1)}\right\}$$
$$Q = \left\{q^{(0)}, q^{(1)}, q^{(2)}\right\}$$

$$P_i^{(0)} = A_1A_2(\overline{T}_i^{+} + \overline{T}_i^{-}); \quad P_i^{(1)} = A_1A_2(h\overline{T}_i^{+} - h\overline{T}_i^{-}), \qquad i = 1, 2, 3$$
$$q^{(n)} = A_1A_2(h^{(n)}\overline{w}^{+} + (-h)^{(n)}\overline{w}^{-}), \quad n = 0, 1, 2$$

Differential matrix operators L_{d} and L_{c}^{*} are given by

$$L_{\mathrm{d}} = L_{\mathrm{d1}}\frac{\partial^2}{\partial\alpha_1^2} + L_{\mathrm{d2}}\frac{\partial^2}{\partial\alpha_2^2} + L_{\mathrm{d3}}\frac{\partial^2}{\partial\alpha_1\partial\alpha_2} + L_{\mathrm{d4}}\frac{\partial}{\partial\alpha_1} + L_{\mathrm{d5}}\frac{\partial}{\partial\alpha_2} + L_{\mathrm{d6}} \tag{28}$$

and

$$L_{\mathrm{c}}^{*} = L_{\mathrm{c1}}^{\mathrm{T}}\frac{\partial^2}{\partial\alpha_1^2} + L_{\mathrm{c2}}^{\mathrm{T}}\frac{\partial^2}{\partial\alpha_2^2} + L_{\mathrm{c3}}^{\mathrm{T}}\frac{\partial^2}{\partial\alpha_1\partial\alpha_2} - L_{\mathrm{c4}}^{\mathrm{T}}\frac{\partial}{\partial\alpha_1} - L_{\mathrm{c5}}^{\mathrm{T}}\frac{\partial}{\alpha_2} + L_{\mathrm{c6}}^{\mathrm{T}} \tag{29}$$

Matrices L_{c} and L_{w} are obtained simply by replacing matrix L_{d} in Eq. (28), respectively. The matrices $L_{\mathrm{d}i}$, $L_{\mathrm{c}i}$, $L_{\mathrm{w}i}$ and L_{ρ} are listed in Appendix A. This completes the derivation of the basic governing equations and the corresponding natural boundary conditions for functionally graded piezoelectric generic shells.

3. Method of solution

The developed high order theory for functionally graded piezoelectric shells is then used to study a simply supported piezoelectric shallow shell subject to applied sinusoidal loads. It can be easily verified that the following displacement and electric potential functions satisfy the simply supported edge boundary conditions,

$$\begin{aligned}
\left\{u_1^{(0)}, u_1^{(1)}\right\} &= \left\{U^{(0)}, U^{(1)}\right\} \cos a\alpha_1 \sin b\alpha_2 \\
\left\{u_2^{(0)}, u_2^{(1)}\right\} &= \left\{V^{(0)}, V^{(1)}\right\} \sin a\alpha_1 \cos b\alpha_2 \\
\left\{u_3^{(0)}, u_3^{(1)}\right\} &= \left\{W^{(0)}, W^{(1)}\right\} \sin a\alpha_1 \sin b\alpha_2
\end{aligned} \tag{30}$$

$$\left\{\varphi^{(0)}, \varphi^{(1)}, \varphi^{(2)}\right\} = \left\{\Psi^{(0)}, \Psi^{(1)}, \Psi^{(2)}\right\} \sin a\alpha_1 \sin b\alpha_2 \tag{31}$$

where $a = m\pi/L_1$, $b = n\pi/L_2$, m and n are integers, L_1 and L_2 are the lengths of the shell in the α_1 and α_2 directions, and the unknown coefficients $U^{(0)}$, $U^{(1)}$, $V^{(0)}$, $V^{(1)}$, $W^{(0)}$, $W^{(1)}$, $\varphi^{(0)}$, $\varphi^{(1)}$, $\varphi^{(2)}$ are to be determined.

We note in passing that the form of the governing equations depends upon the applied electric boundary conditions. Consider first that electric loading is imposed through the surface free charge density. When the following sinusoidal normal traction and surface free charge densities $\overline{T}_3^{\pm} \sin a\alpha_1 \sin b\alpha_2$ and $\overline{w}^{\pm} \sin a\alpha_1 \sin b\alpha_2$ are applied at the major surfaces, a set of algebraic equations regarding the unknown coefficients in Eqs. (30) and (31) can be obtained by substituting Eqs. (30) and (31) into (27), giving

$$[\Gamma]\{x\} = \{F\} \tag{32}$$

where $[\Gamma]$ is a 9×9 symmetric coefficients matrix (see, Appendix B), and $\{x\}$ and $\{F\}$ are, respectively, the unknown displacement and electric potential vector and applied load vector,

$$\begin{aligned}
x &= \left\{U^{(0)}, U^{(1)}, V^{(0)}, V^{(1)}, W^{(0)}, W^{(1)}, \Psi^{(0)}, \Psi^{(1)}, \Psi^{(2)}\right\}^{\mathrm{T}} \\
F &= \left\{0\ 0\ 0\ 0 - A_1A_2(\overline{T}_3^{+} + \overline{T}_3^{-}) - A_1A_2h(\overline{T}_3^{+} - \overline{T}_3^{-}) - A_1A_2(\overline{w}^{+} + \overline{w}^{-}) - A_1A_2h(\overline{w}^{+} - \overline{w}^{-}) - A_1A_2h^2(\overline{w}^{+} + \overline{w}^{-})\right\}^{\mathrm{T}}
\end{aligned} \tag{33}$$

Secondly, consider the electric loading given by the electric potentials acting on the major surfaces. Under such loading conditions, the piezoelectric element functions as actuator. And sinusoidal loadings are assumed on the major surfaces, i.e., $\overline{T}_3^{\pm} \sin a\alpha_1 \sin b\alpha_2$ and $\varphi^{\pm} \sin a\alpha_1 \sin b\alpha_2$. The corresponding algebraic equations related to the unknowns in Eqs. (30) and (31) now read

$$[\widetilde{\Gamma}]\{\widetilde{x}\} = \{\widetilde{F}\} \tag{34}$$

where

$$\begin{aligned}
\{\widetilde{x}\} &= \left\{U^{(0)} U^{(1)} V^{(0)} V^{(1)} W^{(0)} W^{(1)} \Psi^{(0)}\right\}^{\mathrm{T}} \\
\{\widetilde{F}\} &= \left\{0\ 0\ 0\ 0 - A_1A_2\left(\overline{T}_3^{+} + \overline{T}_3^{-}\right) - A_1A_2h\left(\overline{T}_3^{+} - \overline{T}_3^{-}\right) 0\right\}^{\mathrm{T}}
\end{aligned} \tag{35}$$

and $[\widetilde{\Gamma}]$ is a 7×7 symmetric matrix related to $[\Gamma]$ by

$$\begin{aligned}
\widetilde{\Gamma}_{ij} &= \Gamma_{ij}, \qquad i \leqslant 6, \quad j \leqslant 6 \\
\widetilde{\Gamma}_{7j} &= \Gamma_{7j} - \Gamma_{9j}/h^2, \quad j \leqslant 6 \\
\widetilde{\Gamma}_{77} &= \Gamma_{77} - \Gamma_{99}/h^2
\end{aligned} \tag{36}$$

It should be noted that following the above procedure solutions for non-sinusoidal loading can also be obtained using the Fourier series expansion method.

4. Numerical results

To validate the developed high order theory, we first apply it to a simply supported homogeneous piezoelectric shell subjected to sinusoidal mechanical loading on the major surfaces (i.e., the upper and lower surfaces of the shell). Since exact three-dimensional theory of this problem is available (Chen, 1997), a comparison between the present theory solution and exact solution is possible. The homogeneous piezoelectric shell is assumed to be made of PZT-4, with the material constants given (Berlincourt et al., 1964)

$$\begin{aligned} &C_{11} = 13.9, \quad C_{12} = 7.78, \quad C_{13} = 7.43, \quad C_{33} = 11.5, \quad C_{44} = 2.56 \ (10^{10} \text{ Pa}) \\ &e_{31} = -5.2, \quad e_{33} = 15.1, \quad e_{15} = 12.7 \ (\text{C/m}^2), \quad \epsilon_{11} = 6.46, \quad \epsilon_{22} = 5.62 \ (\text{CV/m}) \end{aligned} \tag{37}$$

where the poling direction is along the radial direction.

By assuming the Lame parameters and curvilinear radii to be $A_1 = A_2 = 1$, $R_1 = R_0$, $R_2 = \infty$ where R_0 is the radius of the middle surface of the shell, the developed high order theory can be applied to the circular cylindrical shell. In numerical simulations, the following geometrical parameters for the shell are used: $R_0 = 1$ m, $L_1 = \pi/3$, $L_2 = 4$ m. Two parameters are introduced to describe the thickness effects, namely $S = R_0/2h$, $y = z/2h$. Unless stated otherwise, $S = 5$ and 50 are assumed throughout the following calculations, representing thick and thin shells, respectively. When the homogeneous piezoelectric shell is only subjected to an electric loading in accordance with $\varphi^+ = \overline{\varphi} \sin a\alpha_1 \sin b\alpha_2$ whilst $T_3^{\pm} = 0$, variation of the induced radial displacement (i.e., the transverse displacement) in the radial direction is given in Fig. 2. On the other hand when a mechanical loading in accordance with $T_3^+ = \overline{T} \sin a\alpha_1 \sin b\alpha_2$ with its electric boundary conditions being $\varphi^{\pm} = 0$, distribution of the electric potential in the radial direction is given in Fig. 3. In Figs. 2 and 3, solid and broken lines denote the present high order theory and exact solutions (Chen, 1997), respectively. It can be seen from Figs. 2 and 3 that the high order theory successfully captures the features revealed by the exact solution, that is, the respective linear and parabolic distributions of the resulting radial displacement and electric potential. Notice that the significant change of the transverse displacement in the shell thickness direction suggests a non-negligible transverse normal strain, which has so far been ignored in most published models. For consistent comparison purpose, in Fig. 2,

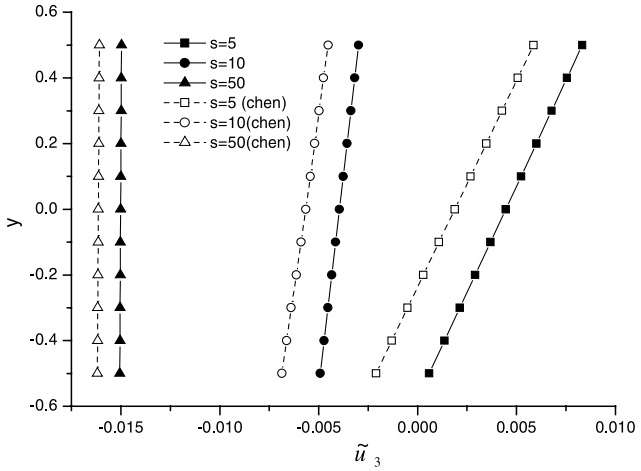

Fig. 2. Radial distribution of the displacement $\widetilde{u}_3$ for homogeneous piezoelectric shells under the loading $\varphi^+ = 1$ V, $T_3^{\pm} = 0$. Results are shown for shells of three thickness ratios ($S = 5$, 10 and 50). Solid and broken lines denote the present high order theory and exact solutions, respectively.

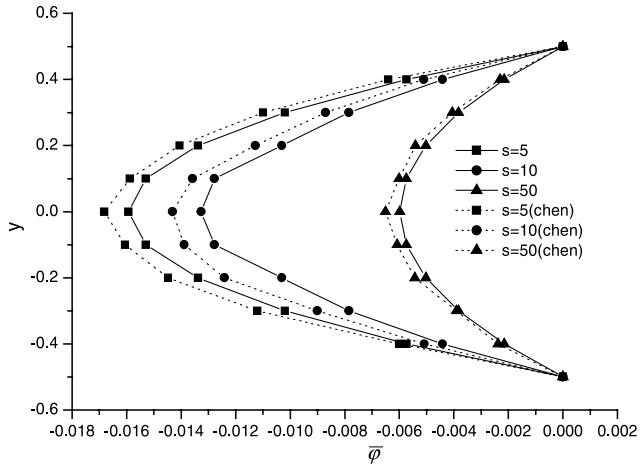

Fig. 3. Radial distribution of the electric potential $\overline{\varphi}$ for homogeneous piezoelectric shells under the loading $T_3^+ = 1$ Pa, $\varphi^{\pm} = 0$. Results are shown for shells of three thickness ratios ($S = 5$, 10 and 50). Solid and broken lines denote the present high order theory and exact solutions, respectively.

$\widetilde{u}_1 = e_{31}/S^2\epsilon_{11}u_1$, $\widetilde{u}_3 = e_{31}/S^2\epsilon_{11}u_3$, $\widetilde{\varphi} = 1/V_0\varphi$ are introduced, and $\overline{u}_1 = C_{11}/2hS^4u_1$, $\overline{u}_3 = C_{11}/2hS^4u_3$, $\overline{\varphi} = e_{31}/2hS^2\varphi$ are introduced in Fig. 3. They will be used in following figures when the applied loading is electric potential on the upper and lower surfaces or surface traction, respectively. Now, consider the shell is made of functionally graded piezoelectric materials, in which only piezoelectric coefficients in Eq. (37) are varied with respect to z while other material properties are the same across the thickness. Two cases are numerically investigated: a linear variation (i.e., $e_{ij}(z) = e_{ij}(1 + z/h)$) and a parabolic variation (i.e., $e_{ij}(z) = 3e_{ij}(1/2 + z/2h)^2$) of the piezoelectric coefficients, with z in the range of $-h$ to h. Note that the

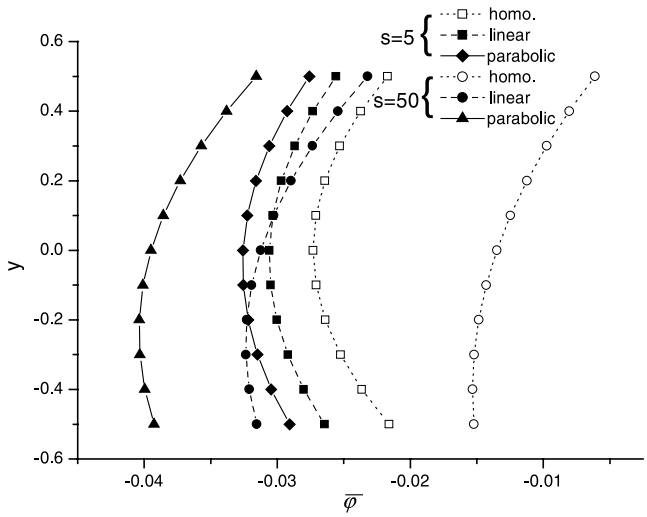

Fig. 4. The electric potential $\overline{\varphi}$ of graded and homogeneous piezoelectric shells for different thickness under loading ($T_3^+ = 1$ Pa, $\overline{w}^{\pm} = 0$).

particular variations of the piezoelectric coefficient are specified to ensure their averaged values along the thickness direction are the same as those of the homogeneous piezoelectric shell.

Figs. 4–7 illustrate the variation of the electric potential $\overline{\varphi}$, displacements (circumferential component $\overline{u}_1$ and radial component $\overline{u}_3$), and the circumferential normal stress σ_{11} induced by the mechanical loading with $\overline{T}_3^+ = 1$ Pa and $\overline{T}_3^- = \overline{D}_r^{\pm} = 0$, where the electric boundary conditions are adopted to model piezoelectric sensors. In each figure, responses of the shell made of three constituent materials, i.e., uniformly (abbreviated as 'homo' in the figures), linearly and parabolically (abbreviated as 'linear' and 'parabolic') varied piezoelectric coefficients, are included for the interests of comparison. It is seen from Fig. 4 that under

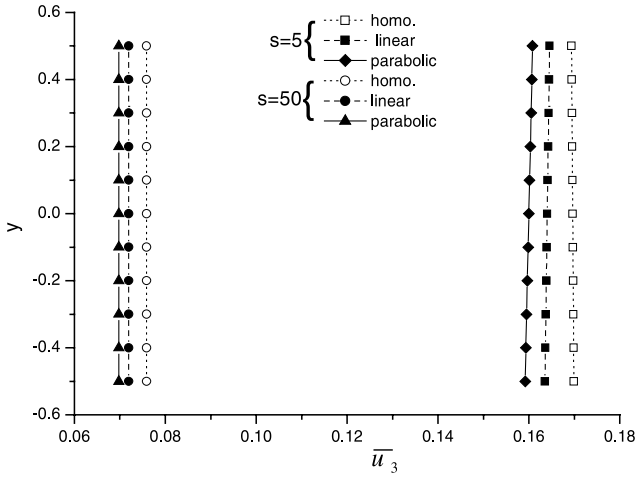

Fig. 5. The out of plane displacement $\overline{u}_3$ of graded and homogeneous piezoelectric shells for different thickness under loading ($T_3^+ = 1$ Pa, $\overline{w}^{\pm} = 0$).

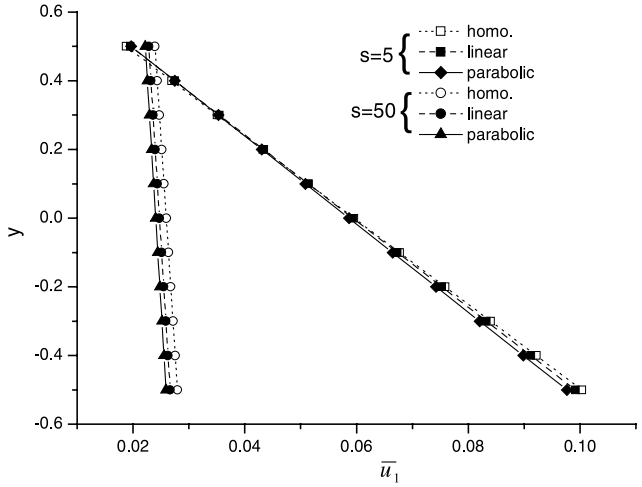

Fig. 6. The in-plane displacement $\overline{u}_1$ of graded and homogeneous piezoelectric shells for different thickness under loading ($T_3^+ = 1$ Pa, $\overline{w}^{\pm} = 0$).

external mechanical loading the induced electric potential for shell with parabolically distributed piezoelectric coefficients is the biggest in magnitude, followed in sequence by those for shells with linearly and uniformly distributed piezoelectric coefficients. In other words, the functionally graded piezoelectric materials are more sensitive to external loading, an important advantage of functionally graded piezoelectric materials over homogeneous ones when acted as sensors. Moreover, the non-linear distribution of the electric potential demonstrates again the necessity for including the second order term in Eq. (12). Note from Fig. 5 that for both thin and thick shells varying the piezoelectric coefficient from uniform to para-

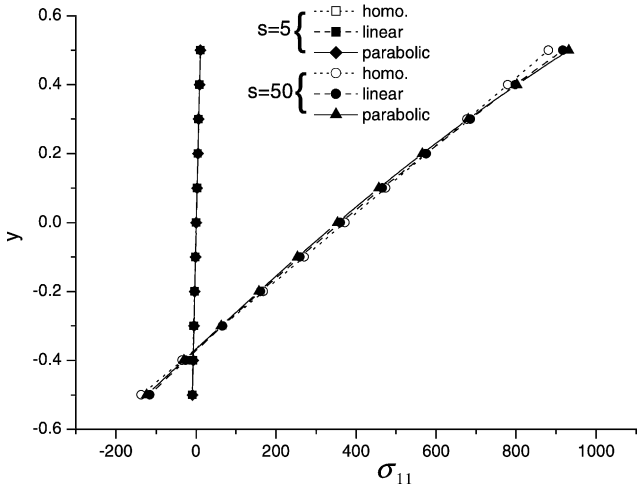

Fig. 7. The in-plane stress σ_{11} of graded and homogeneous piezoelectric shells for different thickness under loading ($T_3^+ = 1$ Pa, $\overline{w}^{\pm} = 0$).

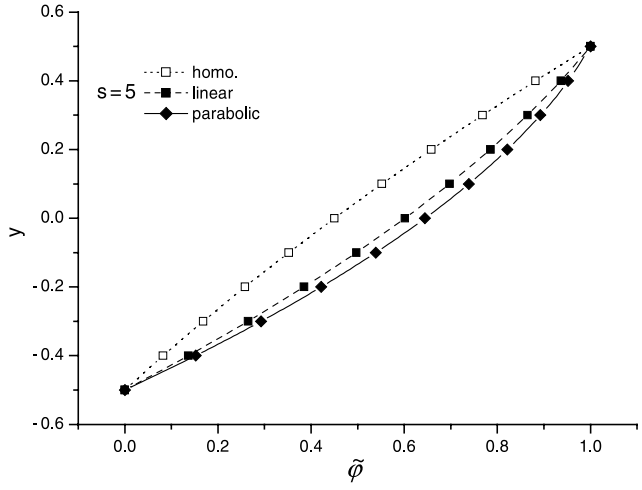

Fig. 8. The electric potential $\widetilde{\varphi}$ of graded and homogeneous piezoelectric shells for different thickness under loading ($\varphi^+ = 1$ V, $T_3^{\pm} = 0$).

bolic distribution in the thickness direction has noticeable effect on the out of plane displacement $\overline{u}_3$. However, the effect is negligible upon the in-plane displacement $\overline{u}_1$ and stress σ_{11}, see Figs. 4–7.

Another important usage of piezoelectric materials is that they can be used as actuators in smart structures. To mimic such situations, the loading with $\overline{T}_3^{\pm} = 0$, $\varphi^- = 0$, and $\overline{\varphi}^+ = 1$ V is applied to the upper and lower surfaces of a moderate thick shell with $S = 5$. The high order theory predicted corresponding responses for the electric potential, displacements, and stress are plotted in Figs. 8–11. Fig. 8 shows the non-linear variation of the electric potential across the shell thickness direction. It is clear from Fig. 8 that the electric potential within functionally graded piezoelectric shells is bigger than that within the homogeneous

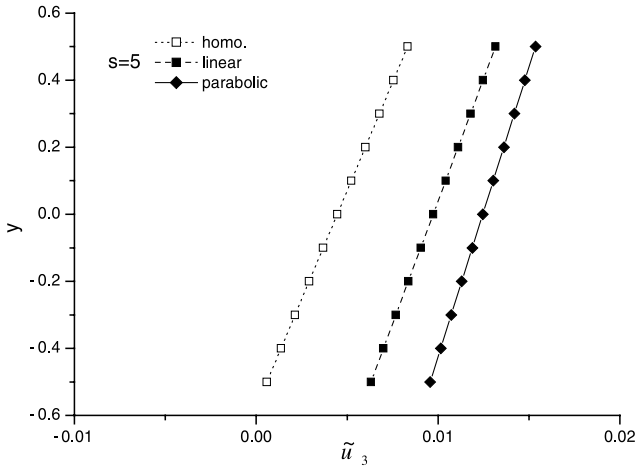

Fig. 9. The out of plane displacement $\widetilde{u}_3$ of graded and homogeneous piezoelectric shells for different thickness under loading ($\varphi^+ = 1$ V, $T_3^{\pm} = 0$).

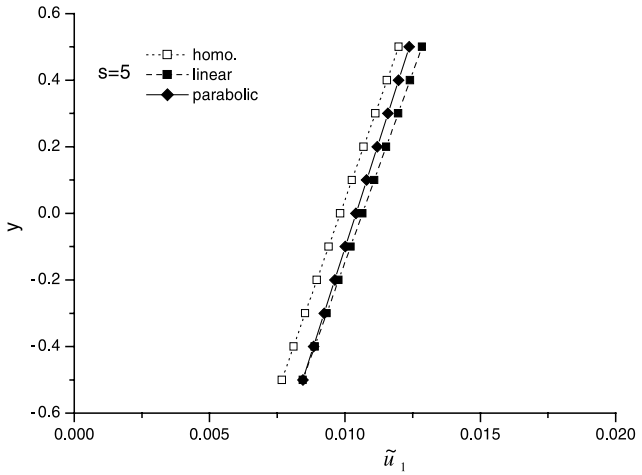

Fig. 10. The in-plane displacement $\widetilde{u}_1$ of graded and homogeneous piezoelectric shells for different thickness under loading ($\varphi^+ = 1$ V, $T_3^{\pm} = 0$).

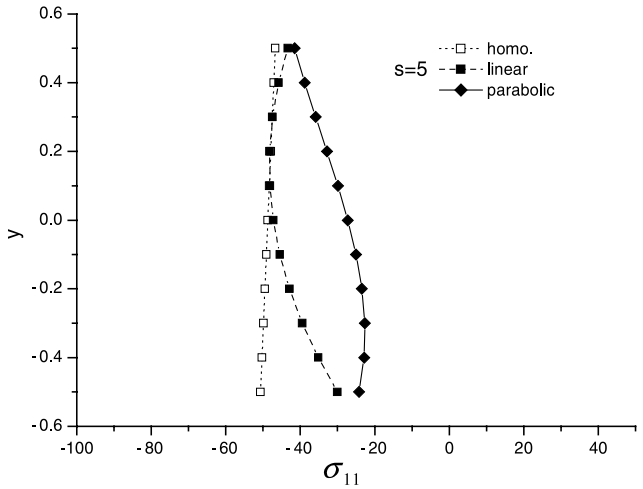

Fig. 11. The in-plane stress σ_{11} of graded and homogeneous piezoelectric shells for different thickness under loading ($\varphi^{+} = 1$ V, $T_3^{\pm} = 0$).

one. This also explains why the induced out of plane displacement $\widetilde{u}_3$ for graded shells is greater (see, Fig. 9). We can thus conclude that the functionally graded piezoelectric materials are better candidates than homogeneous piezoelectric materials when used as constituent materials for actuators. Again, Figs. 10 and 11 reveal that varying the piezoelectric properties has negligible effect on the in-plane displacement $\widetilde{u}_1$ and stress σ_{11}.

5. Conclusion

A high order theory model on the basic governing equations and the corresponding natural boundary conditions for functionally graded piezoelectric generic shells has been derived. The formulae given here can be used to obtain the governing equations for other piezoelectric structures such as beams and plates, treated as degenerated systems of generic shells. With the developed formulations, the electromechanical characteristic of a simply supported inhomogeneous and homogeneous shell is studied. The obtained results agree well with available exact solutions. The assumed transverse normal strain and parabolic variation of the electric potential in the high order theory are found to be essential for accurate modeling. The sensing and actuating mechanisms of a functionally graded piezoelectric shell are investigated. The obtained results show that, in terms of sensing and actuating, the functionally graded piezoelectric materials are superior to homogeneous piezoelectric materials.

Acknowledgements

The authors would like to thank the financial support of the National Natural Science Foundation of China (No. 10132010) and the Department of Education of China through the Funding Project for Authors of National Distinguished PhD Thesis (No. 200129).

Appendix A

The matrices appearing in Eq. (28) are expressed as follows:

Matrix L_{d1}:

$$L_{d1}(1,1) = A_{11}A_2/A_1, \quad L_{d1}(1,2) = L_{d1}(2,1) = B_{11}A_2/A_1, \quad L_{d1}(2,2) = D_{11}A_2/A_1$$
$$L_{d1}(3,3) = A_{66}A_2/A_1, \quad L_{d1}(3,4) = L_{d1}(4,3) = B_{66}A_2/A_1, \quad L_{d1}(4,4) = D_{66}A_2/A_1$$
$$L_{d1}(5,5) = A_{55}A_2/A_1, \quad L_{d1}(5,6) = L_{d1}(6,5) = B_{55}A_2/A_1, \quad L_{d1}(6,6) = D_{55}A_2/A_1$$

The other components are zero.

Matrix L_{d2}:

$$L_{d2}(1,1) = A_{66}A_1/A_2, \quad L_{d2}(1,2) = L_{d2}(2,1) = B_{66}A_1/A_2, \quad L_{d2}(2,2) = D_{66}A_1/A_2$$
$$L_{d2}(3,3) = A_{22}A_1/A_2, \quad L_{d2}(3,4) = L_{d2}(4,3) = B_{22}A_1/A_2, \quad L_{d2}(4,4) = D_{22}A_1/A_2$$
$$L_{d2}(5,5) = A_{44}A_1/A_2, \quad L_{d2}(5,6) = L_{d2}(6,5) = B_{44}A_1/A_2, \quad L_{d2}(6,6) = D_{44}A_1/A_2$$

The other components are zero.

Matrix L_{d3}:

$$L_{d3}(1,3) = L_{d3}(3,1) = A_{12} + A_{66}, \quad L_{d3}(1,4) = L_{d3}(4,1) = B_{12} + B_{66}$$
$$L_{d3}(2,3) = L_{d3}(3,2) = B_{12} + B_{66}, \quad L_{d3}(2,4) = L_{d3}(4,2) = D_{12} + D_{66}$$

The other components are zero.

Matrix L_{d4}:

$$L_{d4}(1,5) = -L_{d4}(5,1) = A_2(A_{11}/R_1 + A_{12}/R_2 + A_{55}/R_1)$$
$$L_{d4}(1,6) = -L_{d4}(6,1) = A_2(A_{13} + B_{11}/R_1 + B_{12}/R_2 + B_{55}/R_1)$$
$$L_{d4}(2,5) = -L_{d4}(5,2) = A_2(B_{11}/R_1 + B_{12}/R_2 + B_{55}/R_1 - A_{55})$$
$$L_{d4}(2,6) = -L_{d4}(6,2) = A_2(B_{13} + D_{11}/R_1 + D_{12}/R_2 - B_{55} + D_{55}/R_1)$$

The other components are zero.

Matrix L_{d5}:

$$L_{d5}(3,5) = -L_{d5}(5,3) = A_1(A_{12}/R_1 + A_{22}/R_2 + A_{44}/R_2)$$
$$L_{d5}(3,6) = -L_{d5}(6,3) = A_1(A_{23} + B_{12}/R_1 + B_{22}/R_2 + B_{44}/R_2)$$
$$L_{d5}(4,5) = -L_{d5}(5,4) = A_1(B_{12}/R_1 + B_{22}/R_2 + B_{44}/R_2 - A_{44})$$
$$L_{d5}(4,6) = -L_{d5}(6,4) = A_1(B_{23} + D_{12}/R_1 + D_{22}/R_2 + D_{44}/R_2 - B_{44})$$

The other components are zero.

Matrix L_{d6}:

$$L_{d6}(1,1) = -A_{55}A_1A_2/R_1^2, \quad L_{d6}(1,2) = L_{d6}(2,1) = A_{55}A_1A_2/R_1 - B_{55}A_1A_2/R_1^2$$
$$L_{d6}(2,2) = -2B_{55}A_1A_2/R_1 - D_{55}A_1A_2/R_1^2 - A_{55}A_1A_2$$
$$L_{d6}(3,3) = -A_{44}A_1A_2/R_2^2$$
$$L_{d6}(3,4) = L_{d6}(4,3) = A_{44}A_1A_2/R_2 - B_{44}A_1A_2/R_2^2$$
$$L_{d6}(4,4) = 2B_{44}A_1A_2/R_2 - D_{44}A_1A_2/R_2^2 - A_{44}A_1A_2$$
$$L_{d6}(5,5) = -A_{11}A_1A_2/R_1^2 - 2A_{12}A_1A_2/(R_1R_2) - A_{22}A_1A_2/R_2^2$$
$$L_{d6}(5,6) = -A_{11}A_1A_2/R_1^2 - 2A_{12}A_1A_2/(R_1R_2) - A_{22}A_1A_2/R_2^2$$

The other components are zero.

Matrix L_{c1}:

$$L_{c1}(5,1) = P_{15}A_2/A_1, L_{c1}(5,2) = L_{c1}(6,1) = Q_{15}A_2/A_1$$
$$L_{c1}(5,3) = L_{c1}(6,2) = R_{15}A_2/A_1, L_{c1}(6,3) = H_{15}A_2/A_1$$

The other components are zero.

Matrix L_{c2}:

$$L_{c2}(5,1) = P_{24}A_1/A_2, L_{c2}(5,2) = L_{c2}(6,1) = Q_{24}A_1/A_2$$
$$L_{c2}(5,3) = L_{c2}(6,2) = R_{24}A_1/A_2, L_{c2}(6,3) = H_{24}A_1/A_2$$

The other components are zero.

Matrix L_{c4}:

$$L_{c4}(1,1) = P_{15}A_2/R_1, L_{c4}(1,2) = (P_{31} + Q_{15}/R_1)A_2, L_{c4}(1,3) = (2Q_{31} + R_{15}/R_1)A_2$$
$$L_{c4}(2,1) = (-P_{15} + Q_{15}/R_1)A_2, L_{c4}(2,2) = (Q_{31} - Q_{15} + R_{15}/R_1)A_2$$
$$L_{c4}(2,2) = (2R_{31} - R_{15} + H_{15}/R_1)A_2,$$

The other components are zero.

Matrix L_{c5}:

$$L_{c5}(3,1) = P_{24}A_1/R_2, L_{c4}(3,2) = (P_{32} + Q_{24}/R_2)A_1, L_{c4}(3,3) = (2Q_{32} + R_{24}/R_2)A_1$$
$$L_{c4}(4,1) = (-P_{24} + Q_{24}/R_2)A_1, L_{c4}(4,2) = (Q_{32} - Q_{24} + R_{24}/R_2)A_1$$
$$L_{c4}(4,3) = (2R_{32} - R_{24} + H_{24}/R_2)A_1$$

The other components are zero.

Matrix L_{c6}:

$$L_{c6}(5,2) = -(P_{31}/R_1 + P_{32}/R_2)A_1A_2, L_{c6}(5,3) = -2(Q_{31}/R_1 + Q_{32}/R_2)A_1A_2$$
$$L_{c6}(6,2) = -(Q_{31}/R_1 + Q_{32}/R_2 + P_{33})A_1A_2, L_{c6}(6,3) = -2(R_{31}/R_1 + R_{32}/R_2 + Q_{33})A_1A_2$$

The other components are zero.

Matrix L_{w1}:

$$L_{w1} = \begin{bmatrix} -K_{11}A_2/A_1 & -L_{11}A_2/A_1 & -M_{11}A_2/A_1 \\ -L_{11}A_2/A_1 & -M_{11}A_2/A_1 & -N_{11}A_2/A_1 \\ -M_{11}A_2/A_1 & -N_{11}A_2/A_1 & -O_{11}A_2/A_1 \end{bmatrix}$$

Matrix L_{w2}:

$$L_{w2} = \begin{bmatrix} -K_{22}A_1/A_2 & -L_{22}A_1/A_2 & -M_{22}A_1/A_2 \\ -L_{22}A_1/A_2 & -M_{22}A_1/A_2 & -N_{22}A_1/A_2 \\ -M_{22}A_1/A_2 & -N_{22}A_1/A_2 & -O_{22}A_1/A_2 \end{bmatrix}$$

Matrix $L_{w3} = L_{w4} = L_{w5} = 0$.

Matrix L_{w6}:

$$L_{w6} = \begin{bmatrix} 0 & 0 & 0 \\ 0 & K_{33}A_1A_2 & 2L_{33}A_1A_2 \\ 0 & 2L_{33}A_1A_2 & 4M_{33}A_1A_2 \end{bmatrix}$$

Matrix L_ρ:

$$L_\rho = \begin{bmatrix} \rho^{(0)} & \rho^{(1)} & 0 & 0 & 0 & 0 \\ \rho^{(1)} & \rho^{(2)} & 0 & 0 & 0 & 0 \\ 0 & 0 & \rho^{(0)} & \rho^{(1)} & 0 & 0 \\ 0 & 0 & \rho^{(1)} & \rho^{(2)} & 0 & 0 \\ 0 & 0 & 0 & 0 & \rho^{(0)} & \rho^{(1)} \\ 0 & 0 & 0 & 0 & \rho^{(1)} & \rho^{(2)} \end{bmatrix}$$

Appendix B

$$\begin{aligned}
\Gamma_{11} &= -\left(a^2A_2/A_1A_{11} + b^2A_1/A_2A_{66} + A_1A_2A_{55}/R_1^2\right)\\
\Gamma_{12} &= A_1A_2A_{55}/R_1 - a^2A_2/A_1B_{11} - b^2A_1/A_2B_{66} - A_1A_2B_{55}/R_1^2\\
\Gamma_{13} &= -ab(A_{12} + A_{66})\\
\Gamma_{14} &= -ab(B_{12} + B_{66})\\
\Gamma_{15} &= aA_2(A_{11}/R_1 + A_{12}/R_2 + A_{55}/R_1)\\
\Gamma_{16} &= aA_2(A_{13} + B_{11}/R_1 + B_{12}/R_2 + B_{55}/R_1)\\
\Gamma_{17} &= aA_2P_{15}/R_1\\
\Gamma_{18} &= aA_2(P_{31} + Q_{15}/R_1)\\
\Gamma_{19} &= aA_2(R_{15}/R_1 + 2Q_{31})\\
\Gamma_{22} &= -\left(a^2A_2/A_1D_{11} + b^2A_1/A_2D_{66} + A_1A_2D_{55}/R_1^2 + A_1A_2A_{55} - 2B_{55}A_1A_2/R_1^2\right)\\
\Gamma_{23} &= -ab(B_{12} + B_{66})\\
\Gamma_{24} &= -ab(D_{12} + D_{66})\\
\Gamma_{25} &= aA_2(-A_{55} + B_{11}/R_1 + B_{12}/R_2 + B_{55}/R_1)\\
\Gamma_{26} &= aA_2(D_{11}/R_1 + D_{12}/R_2 + D_{55}/R_1 + B_{13} - B_{55})\\
\Gamma_{27} &= aA_2(-P_{15} + Q_{15}/R_1)\\
\Gamma_{28} &= -aA_2(R_{15}/R_1 + Q_{31} - Q_{15})\\
\Gamma_{29} &= aA_2(2R_{31} - R_{15} + H_{15}/R_1)\\
\Gamma_{33} &= -\left(a^2A_2/A_1A_{66} + b^2A_1/A_2A_{22} + A_1A_2A_{44}/R_2^2\right)\\
\Gamma_{34} &= A_1A_2A_{44}/R_2 - a^2A_2/A_1B_{66} - b^2A_1/A_2B_{22} - A_1A_2B_{44}/R_2^2\\
\Gamma_{35} &= bA_1(A_{12}/R_1 + A_{22}/R_2 + A_{44}/R_2)\\
\Gamma_{36} &= bA_1(A_{23} + B_{12}/R_1 + B_{22}/R_2 + B_{44}/R_2)\\
\Gamma_{37} &= bA_1P_{24}/R_2\\
\Gamma_{38} &= bA_1(P_{32} + Q_{24}/R_2)\\
\Gamma_{39} &= bA_1(R_{24}/R_2 + 2Q_{32})\\
\Gamma_{44} &= -a^2A_2/A_1D_{66} - b^2A_1/A_2D_{22} - A_{44}A_1A_2 + 2B_{44}A_1A_2/R_2 - A_1A_2D_{44}/R_2^2\\
\Gamma_{45} &= bA_1(-A_{44} + B_{12}/R_1 + B_{22}/R_2 + B_{22}/R_2)\\
\Gamma_{46} &= bA_1(D_{12}/R_1 + D_{22}/R_2 + D_{44}/R_2 + B_{23} - B_{44})\\
\Gamma_{47} &= bA_1(-P_{24} + Q_{24}/R_2)
\end{aligned}$$

$$
\begin{aligned}
\Gamma_{48} &= bA_1(Q_{32} - Q_{24} + R_{24}/R_2)\\
\Gamma_{49} &= bA_1(2R_{32} - R_{24} + H_{24}/R_2)\\
\Gamma_{55} &= -\left(a^2A_2/A_1A_{55} + b^2A_1/A_2A_{44} + A_1A_2/R_1^2A_{11} + 2A_1A_2/(R_1R_2)A_{12} + A_1A_2/R_2^2A_{22}\right)\\
\Gamma_{56} &= -(a^2A_2/A_1B_{55} + b^2A_1/A_2B_{44} + A_1A_2/R_1A_{13} + A_1A_2/R_2A_{23} + A_1A_2/R_1^2B_{11}\\
&\quad + 2A_1A_2/(R_1R_2)B_{12} + A_1A_2/R_2^2B_{22})\\
\Gamma_{57} &= -\left(a^2A_2/A_1P_{15} + b^2A_1/A_2P_{24}\right)\\
\Gamma_{58} &= -\left(a^2A_2/A_1Q_{15} + b^2A_1/A_2Q_{24} + A_1A_2/R_1P_{31} + A_1A_2/R_2P_{32}\right)\\
\Gamma_{59} &= -\left(a^2A_2/A_1R_{15} + b^2A_1/A_2R_{24} + 2A_1A_2/R_1Q_{31} + 2A_1A_2/R_2Q_{32}\right)\\
\Gamma_{66} &= (a^2A_2/A_1D_{55} + b^2A_1/A_2D_{44} + A_1A_2/R_1^2D_{11} + 2A_1A_2/(R_1R_2)D_{12} + A_1A_2/R_2^2D_{22}\\
&\quad + 2A_1A_2/R_1B_{13} + 2A_1A_2/R_2B_{23} + A_1A_2C_{33}\\
\Gamma_{67} &= -\left(a^2A_2/A_1Q_{15} + b^2A_1/A_2Q_{24}\right)\\
\Gamma_{68} &= -\left(a^2A_2/A_1R_{15} + b^2A_1/A_2R_{24} + A_1A_2/R_1Q_{31} + A_1A_2/R_2Q_{32} + A_1A_2P_{33}\right)\\
\Gamma_{69} &= -\left(a^2A_2/A_1H_{15} + b^2A_1/A_2H_{24} + 2A_1A_2/R_1R_{31} + 2A_1A_2/R_2R_{32} + 2A_1A_2Q_{33}\right)\\
\Gamma_{77} &= a^2A_2/A_1K_{11} + b^2A_1/A_2K_{22}\\
\Gamma_{78} &= a^2A_2/A_1L_{11} + b^2A_1/A_2L_{22}\\
\Gamma_{79} &= a^2A_2/A_1M_{11} + b^2A_1/A_2M_{22}\\
\Gamma_{88} &= a^2A_2/A_1M_{11} + b^2A_1/A_2M_{22} + K_{33}A_1A_2\\
\Gamma_{89} &= a^2A_2/A_1N_{11} + b^2A_1/A_2N_{22} + 2L_{33}A_1A_2\\
\Gamma_{99} &= a^2A_2/A_1O_{11} + b^2A_1/A_2O_{22} + 4M_{33}A_1A_2.
\end{aligned}
$$

References

Berlincourt, D.A., Curran, D.R., Jaffe, H., 1964. Piezoelectric and piezomagnetic materials and their function in transducers. In: Mason, W.P. (Ed.), Physical Acoustics, vol. 1. Academic Press, New York, pp. 169–270.

Bisegna, P., Caruso, G., 2001. Evaluation of higher-order theories of piezoelectric plates in bending and in stretching. Int. J. Solid Struct. 38, 8805–8830.

Bisegna, P., Maceri, F., 1996. An exact three-dimensional solution for simply supported rectangular piezoelectric plates. ASME J. Appl. Mech. 63, 628–638.

Chen, C.Q., 1997. Electromechanical properties of piezoelectric materials and structures—Theory and Application, Xi'an Jiaotong University PhD Thesis.

Chen, C.Q., Shen, Y.P., Wang, X.M., 1996. Exact solution of orthotropic cylindrical shell with piezoelectric layers under cylindrical bending. Int. J. Solid Struct. 33, 4481–4491.

Chen, C.Q., Shen, Y.P., Liang, X., 1999. Three dimensional analysis of piezoelectric circular cylindrical shell of finite length. Acta Mech. 134, 235–249.

Heyliger, p., 1997. Exact solutions for simply supported laminated piezoelectric plates. ASME J. Appl. Mech. 64, 299–306.

Kim, S., Jones, J.D., 1991. Optimal design of piezoelectric actuators for active noise and vibration control. AIAA J. 29, 2047–2053.

Koizumi, M., 1993. The concept of FGM. Ceram. Trans. Funct. Gradient. Mater. 34, 3–10.

Lee, J.S., Jiang, L., 1996. Exact electroelastic analysis of piezoelectric laminae via state space approach. Int. J. Solid Struct. 33, 977–990.

Marcus, M.A., 1981. Depth dependence of piezoelectric activity in poly(vinylidene fluoride) transducers: control and measurement. J. Appl. Phys. 52, 6273–6278.

Miller, S.E., Abramovich, H., 1995. A self-sensing piezolaminated actuator model for shells using a first shear deformation theory. J. Intell. Mater. Syst. Struct. 6, 624–638.

Niino, M., 1990. Development of functionally gradient material. J. Jpn. Soc. Power Metall. 37, 146–241.

Pagano, N.J., 1970. Exact solutions for rectangular bi-directional composites and sandwich plates. J. Compos. Mater. 4, 20–34.
Reddy, J.N., Cheng, Z.Q., 2001. Three-dimensional solutions of smart functionally graded plates. ASME J. Appl. Mech. 68, 234–241.
Reddy, J.N., Chin, C.D., 1998. Thermomechanical analysis of functionally graded cylinders and plates. J. Therm. Stress. 21, 593–626.
Rivory, J.F., Hasen, C.H., Pan, J., 1994. Further studies of the dynamic response of a simply supported beam excited by a pair of out-of-phase piezoelectric actuators. J. Intell. Mater. Syst. Struct. 5, 654–664.
Sosa, H.A., 1992. On the modelling of piezoelectric laminated structures. Mech. Res. Commun. 19, 541–546.
Tzou, H.S., Gadre, M., 1989. Theoretical analysis of a multi-layered thin shell coupled with piezoelectric actuators for distributed vibration controls. J. Sound Vib. 132, 349–435.
Tzou, H.S., Howard, R.V., 1994. A piezothermoelastic thin shell theory applied to active structures. ASME J. Vib. Acoust. 116, 295–302.
Wang, J., Yang, J.S., 2000. Higher-order theories of piezoelectric plates and applications. Appl. Mech. Rev. 53, 87–99.
Wu, C.C.M., Kahn, M., Moy, W., 1996. Piezoelectric ceramics with functional gradients: a new application in material design. J. Americ. Ceram. Soc. 79, 809–812.
Xu, K., Noor, A.K., Tang, Y.Y., 1997. Three-dimensional solutions for coupled thermoelectroelastic response of multilayered plates. Comput. Meth. Appl. Mech. Eng. 19, 541–546.
Yang, J.S., 1999. Equations for thick elastic plates with partially electroded piezoelectric actuators and higher order electric fields. Smart Mater. Struct. 8, 73–82.
Zhu, X.H., Meng, Z.Y., 1996. Operational principle, fabrication and displacement characteristics of a functionally gradient piezoelectric ceramic actuator. Sensors Actuators A 48, 169–173.